



HAL
open science

Underestimation of Methane Emissions From the Sudd Wetland: Unraveling the Impact of Wetland Extent Dynamics

Bogang Dong, Shushi Peng, Gang Liu, Tianjiao Pu, Cynthia Gerlein-safdi,
Catherine Prigent, Xin Lin

► **To cite this version:**

Bogang Dong, Shushi Peng, Gang Liu, Tianjiao Pu, Cynthia Gerlein-safdi, et al.. Underestimation of Methane Emissions From the Sudd Wetland: Unraveling the Impact of Wetland Extent Dynamics. *Geophysical Research Letters*, 2024, 51 (16), 10.1029/2024gl110690 . hal-04679028

HAL Id: hal-04679028

<https://hal.science/hal-04679028v1>

Submitted on 27 Aug 2024

HAL is a multi-disciplinary open access archive for the deposit and dissemination of scientific research documents, whether they are published or not. The documents may come from teaching and research institutions in France or abroad, or from public or private research centers.

L'archive ouverte pluridisciplinaire **HAL**, est destinée au dépôt et à la diffusion de documents scientifiques de niveau recherche, publiés ou non, émanant des établissements d'enseignement et de recherche français ou étrangers, des laboratoires publics ou privés.

Geophysical Research Letters®









RESEARCH LETTER

10.1029/2024GL110690

Underestimation of Methane Emissions From the Sudd Wetland: Unraveling the Impact of Wetland Extent Dynamics

Key Points:

- Extended monthly inundation maps across the Sudd wetland for 2003–2022
- Rapid growth of the Sudd wetland extent for 2019–2022 driven by upstream precipitation
- Underestimation of methane emissions from the Sudd wetland due to the inadequate characterization of wetland extent

Bogang Dong¹ , Shushi Peng¹ , Gang Liu¹, Tianjiao Pu² , Cynthia Gerlein-Safdi² , Catherine Prigent³ , and Xin Lin⁴ 

¹Laboratory for Earth Surface Processes, College of Urban and Environmental Sciences, Sino-French Institute for Earth System Science, Peking University, Beijing, China, ²Department of Civil and Environmental Engineering, UC Berkeley, Berkeley, CA, USA, ³LERMA, Paris Observatory, CNRS, PSL, Paris, France, ⁴Laboratoire des Sciences du Climat et de l'Environnement, LSCE/IPSL, CEA-CNRS-UVSQ, Université Paris-Saclay, Gif-sur-Yvette, France

Supporting Information:

Supporting Information may be found in the online version of this article.

Correspondence to:

S. Peng,
speng@pku.edu.cn

Citation:

Dong, B., Peng, S., Liu, G., Pu, T., Gerlein-Safdi, C., Prigent, C., & Lin, X. (2024). Underestimation of methane emissions from the Sudd wetland: Unraveling the impact of wetland extent dynamics. *Geophysical Research Letters*, 51, e2024GL110690. <https://doi.org/10.1029/2024GL110690>

Received 6 JUN 2024
Accepted 19 AUG 2024

Author Contributions:

Conceptualization: Bogang Dong, Shushi Peng, Xin Lin
Methodology: Bogang Dong, Shushi Peng
Resources: Shushi Peng, Gang Liu, Tianjiao Pu, Cynthia Gerlein-Safdi, Catherine Prigent
Writing – original draft: Bogang Dong
Writing – review & editing: Shushi Peng, Cynthia Gerlein-Safdi, Catherine Prigent, Xin Lin

Abstract Tropical wetlands account for ~20% of the global total methane (CH₄) emissions, but uncertainties remain in emission estimation due to the inaccurate representation of wetland spatiotemporal variations. Based on the latest satellite observational inundation data, we constructed a model to map the long-term time series of wetland extents over the Sudd floodplain, which has recently been identified as an important source of wetland CH₄ emissions. Our analysis reveals an annual, total wetland extent of $5.73 \pm 2.05 \times 10^4$ km² for 2003–2022, with a notable accelerated expansion rate of 1.19×10^4 km² yr⁻¹ during 2019–2022 driven by anomalous upstream precipitation patterns. We found that current wetland products generally report smaller wetland areas, resulting in a systematic underestimation of wetland CH₄ emissions from the Sudd wetland. Our study highlights the pivotal role of comprehensively characterizing the seasonal and interannual dynamics of wetland extent to accurately estimate CH₄ emissions from tropical floodplains.

Plain Language Summary Methane (CH₄) plays an important role in global warming. About one-fifth of global CH₄ emissions come from tropical wetlands, with the Sudd wetland in tropical Africa presenting as a hotspot for CH₄ emissions. In this study, we generate a monthly wetland map series based on the latest satellite observation for the Sudd wetland. Our results show that wetland area dynamics present large seasonal and interannual variabilities. However, current widely used wetland products tend to indicate smaller sizes and variations of wetlands, which might lead to the underestimation of wetland CH₄ emissions. We point out that refined maps of tropical wetlands can help reduce the uncertainties of CH₄ emission estimations.

1. Introduction

Methane (CH₄) is the second most important anthropogenic greenhouse gas after carbon dioxide, accounting for 15%–35% of the global radiative forcing from greenhouse gases (IPCC, 2021). The global atmospheric CH₄ growth rate has been accelerating since 2014, reaching a record-breaking level of 17.9 ppb yr⁻¹ in 2021 (Lan et al., 2024). Accounting for ~20% of the global total (natural and anthropogenic) sources, CH₄ emissions from tropical wetlands are thought to dominate the interannual variability in global atmospheric CH₄ growth (Kirschke et al., 2013; Parker et al., 2018; Poulter et al., 2017; Saunio et al., 2020a). In particular, tropical Africa, with its extensive distribution of wetlands (e.g., the Sudd, the Congo, and the Nigeria), is dominant in determining the variation of tropical emissions. These variations accounted for more than 80% of the observed global atmospheric growth rate for 2010–2019 (Feng et al., 2022). The spatial and temporal distribution of wetlands represents one of the most critical factors determining the location and timing of tropical wetland CH₄ emissions, particularly in tropical floodplains where wetland extents present substantial seasonal and interannual variabilities that depend on variations in water balance and local topography (Parker et al., 2018; Z. Zhang et al., 2021a). Therefore, precise mapping of wetland extent in tropical floodplains, especially in Africa, is crucial for improving our understanding of the global CH₄ budget and its potential changes under future climate scenarios.

Located in the central part of South Sudan, the Sudd wetland represents one of the largest floodplain wetlands in the world (Figure 1a). It receives inflows primarily from the White Nile, which originates from Lake Victoria to the south, and several seasonal streams originating from the west and east (Figure 1a). In 2006, the Sudd wetland was officially recognized as a Ramsar Wetland of International Importance with a designated area of 57,000 km².

© 2024. The Author(s).

This is an open access article under the terms of the [Creative Commons Attribution-NonCommercial-NoDerivs License](https://creativecommons.org/licenses/by/4.0/), which permits use and distribution in any medium, provided the original work is properly cited, the use is non-commercial and no modifications or adaptations are made.

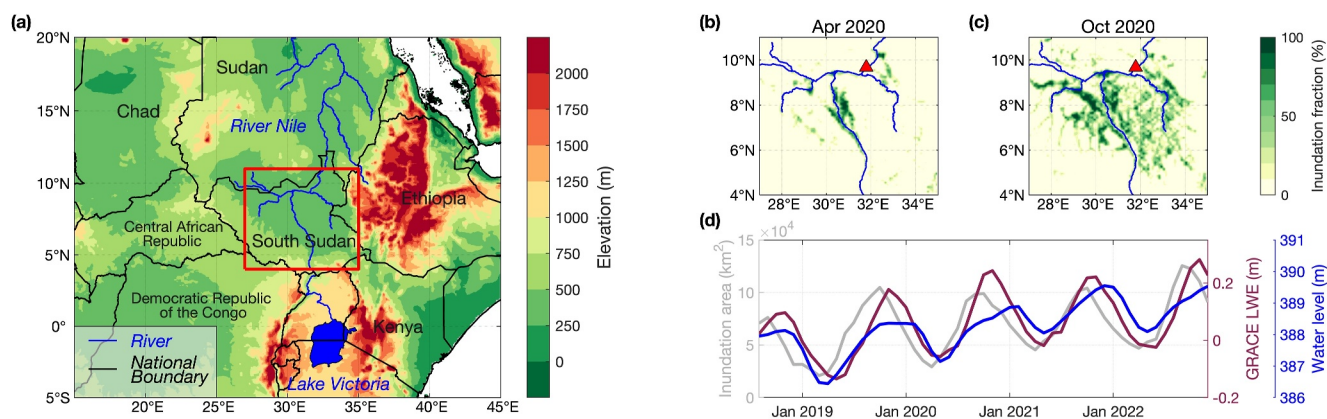


Figure 1. (a) Location of the Sudd region (red rectangle, 4°–11°N, 27°–35°E) and topographic map of the surrounding area. (b–c) Berkeley-RWAWC inundation extents in the Sudd region for April 2020 and October 2020. (d) Comparison of the variations of Berkeley-RWAWC total inundation area, Gravity Recovery and Climate Experiment (GRACE) liquid water equivalent (LWE) anomaly averaged across the Sudd region, and the water level of a virtual station of the White Nile (marked with red triangles in (b) and (c)) from August 2018 to December 2022. The time series of river water level (based on satellite altimetry) is calculated by a 3-month moving average.

However, due to seasonal flooding, the extent of the Sudd wetland varies greatly within a year (Figures 1b and 1c). During flooding seasons, as the White Nile approaches South Sudan, the water levels overcome the comparatively shallow riverbanks, resulting in overflows from the main channel into the adjacent swamps and seasonally flooded areas (Sutcliffe & Parks, 1999). This gives rise to a complex network comprising river channels, lagoons, and inundated areas (Figure 1c). In contrast, during dry seasons, water mainly flows through meandering river channels without extensive overflow (Figure 1b). The extensively distributed floodplains make South Sudan a hotspot for CH₄ emissions in tropical Africa, with wetland emissions accounting for ~60% of the total emissions from the Sudd region (Lunt et al., 2019). However, recent studies pointed out that wetland CH₄ emission models perform poorly at capturing the distributions and the seasonal cycles of wetland CH₄ emissions in South Sudan compared to satellite observation (Lunt et al., 2019, 2021; Pandey et al., 2021; Parker et al., 2022). This poor performance is mainly attributed to the inadequate representation of wetland extent and its dynamics (Bloom et al., 2017).

In this study, we developed a statistic model utilizing a robust observational inundation data set during the period 2018–2022 and associated satellite-based water storage and precipitation data. We used this model to reconstruct monthly maps for 2003–2022 across the Sudd wetland and then applied this new wetland extent data to improve the estimation of wetland CH₄ emissions. Following Gerlein-Safdi et al. (2021), we defined the Sudd region within the geographic bounds of 4–11°N, 27–35°E.

2. Materials and Methods

2.1. Satellite-Based Wetland Extent Data

Optical satellite-based maps tend to underestimate wetland extent in the tropics due to the obstruction of thick clouds and dense vegetation (Martins et al., 2018). Producing a cloud-free map necessitates the aggregation of data over several months, leading to a loss of temporal resolution (Hardy et al., 2023). Working at an L-band frequency of 1.575 GHz to avoid attenuation and scattering by clouds or vegetation canopies, the Cyclone Global Navigation Satellite System (CYGNSS) constellation provides possibilities to monitor inland waterbody with high temporal granularity (Ruf et al., 2018). The CYGNSS-based approach has proved to be highly sensitive to seasonal variations in inland surface water (Gerlein-Safdi & Ruf, 2019; Ruf et al., 2018; Zeiger et al., 2022), and has been widely used for detecting wetland extent and flooding inundation (Chew et al., 2023; Gerlein-Safdi et al., 2021).

Here, we used the UC Berkeley Random Walk Algorithm WaterMask from the CYGNSS (Berkeley-RWAWC) data set as the observed wetland extent for our model (Pu et al., 2024). This product provides monthly binary surface water extent maps at a resolution of 0.01° × 0.01° since August 2018 and demonstrates high agreement with other optical data in the Sudd wetland (Hardy et al., 2023; Pu et al., 2024). The spatial patterns of inundation

regions for April and October 2020 are presented in Figures 1b and 1c. For our statistic model, we calculated the wetland fraction at a resolution of $0.5^\circ \times 0.5^\circ$ from the Berkeley-RWAWC data set.

2.2. Input Data for Our Statistic Model

We used the Gravity Recovery and Climate Experiment (GRACE) and its follow-on (GRACE-FO) satellite missions' monthly liquid water equivalent (LWE) anomaly (Landerer et al., 2020; Tapley et al., 2004) and the Multi-Source Weighted-Ensemble Precipitation (MSWEP) v2.8 monthly precipitation (Beck et al., 2019) as predictors for wetland extent. The variations of LWE are consistent with the seasonal cycle of observed wetland extent (Figure 1d), and the precipitation data was used to improve the inadequate representation of LWE with a coarse spatial resolution of about $3^\circ \times 3^\circ$ (Gou & Soja, 2024). All LWE and precipitation data were resampled to $0.5^\circ \times 0.5^\circ$ using the nearest sampling and spatial averaging, respectively.

The GRACE and GRACE-FO (hereafter GRACE) missions provide opportunities for continuously monitoring the changes in global terrestrial water storage by measuring gravity field variations (Tapley et al., 2019). Here we used GRACE Level-3 mascon products from January 2003 to January 2023. The 13-month gap between the two missions and 20 additional missing months were filled by the singular spectrum analysis gap-filling technique developed by Yi and Sneeuw (2021).

The MSWEP product utilizes a combination of satellite, gauge, and reanalysis data to produce a consistent data set at a 3-hourly resolution on a $0.1^\circ \times 0.1^\circ$ grid, covering the period from 1979 to the present (Beck et al., 2019). In Africa, it has been reported that the MSWEP product performed best at the monthly and annual timescales among eight widely used precipitation data sets (Mekonnen et al., 2023).

2.3. Construction of Wetland Extent Simulation Model

Following Shen et al. (2017), we constructed a multiple linear regression model to correlate monthly observational inundation fraction with LWE anomaly and both local and regional precipitation at a resolution on a $0.5^\circ \times 0.5^\circ$ grid. The model form is as follows:

$$F_{\text{wet}} = \alpha G + \sum_{i=0}^3 \beta_i P_i + \sum_{j=1}^2 \gamma_j S_j \quad (1)$$

where F_{wet} is the simulated wetland fraction, G refers to GRACE LWE anomaly value; P_0 – P_3 represent the local precipitation for 0–3 months in advance; S_1 and S_2 represent regional precipitation patterns using the singular value decomposition (SVD); α , β , and γ are the corresponding coefficients. For the LWE anomaly, we used data with a 1-month lag since the seasonal cycle of LWE is always 1 month later than that of the observed total wetland extent (Figure 1d). This time-lag phenomenon arises from the temporal delay in the conversion of land-surface water, which directly impacts wetland extent, into terrestrial water (Y. Zhang et al., 2019).

We optimized the simulated model through three steps. First, we tested local precipitation for 0–3 months in advance without considering regional precipitation ($i_{\text{max}} = 0-3$, $\gamma_j = 0$) since previous studies have reported a 1–3 months lag in the seasonality of inundation extent compared to precipitation in the Sudd region (Gerlein-Safdi et al., 2021; Prigent et al., 2020). We selected a maximum value of 3 months for the advance of precipitation ($i_{\text{max}} = 3$) because the corresponding result has the lowest regionally averaged root-mean-square-error (RMSE) and the highest regionally averaged R^2 between simulated and observed wetland fractions when using only local precipitation (Figure S1a in Supporting Information S1).

Second, considering that surface water can be produced by precipitation upstream or in adjacent areas on floodplains, we incorporated regional precipitation impacts (including lag effects) into our simulation model using SVD and determined the optimal value for the regional size (window size). Details of the SVD method can be found in Text S1. To find the best window size for SVD, we tested the value for 1–10, which corresponds to $1.5^\circ \times 1.5^\circ$ – $10.5^\circ \times 10.5^\circ$ of the surrounding area for each grid. We selected a window size of 3 since the corresponding result has a lower regionally averaged RMSE and a higher regionally averaged R^2 compared with using only local precipitation, and there is less improvement with larger window sizes (Figure S1b in Supporting Information S1).

Finally, to avoid overfitting, the simulated maximum wetland fractions were constrained by the observed maximum values, while any simulated wetland fractions below zero were adjusted to zero. For statistical analysis, we employed the function “findchangepts” in MATLAB to find abrupt changes in the annually averaged time series of total wetland extent.

2.4. Site-Based CH₄ Emissions Estimation

We estimated wetland CH₄ emissions by multiplying wetland area with CH₄ emission intensity on a grid scale. For emission intensities, we used data from a random forest upscaling model trained on FLUXNET-CH₄ data (UpCH₄) since it can provide monthly gridded wetland CH₄ emission estimations (McNicol et al., 2023b). Considering the uncertainties of UpCH₄ in the tropics due to limited site samples, we also calculated CH₄ emissions using observational data from a specific FLUXNET-CH₄ site in Brazil's Pantanal wetland (BR-Npw) (Vourlitis et al., 2020). Although the Sudd and the Pantanal are located on two different continents, they are both categorized into riverine seasonally flooded wetlands in the latest Global Lakes and Wetlands Database version 2 (Lehner et al., 2024), and their wetland dynamics are both highly sensitive to precipitation during wet seasons (Gerlein-Safdi et al., 2021). More information about the similarity between these two wetlands is provided in Table S1 in Supporting Information S1.

Specifically, we found the CH₄ fluxes are strongly dependent on the water table depth (WTD) rather than soil temperature (Figure S2 in Supporting Information S1) based on daily observations at site BR-Npw. Furthermore, we observed that the grid-scale (0.25° × 0.25°) root-zone soil moisture from the Global Land Evaporation Amsterdam Model (GLEAM) version 3.8a agrees well with the site-scale WTD in seasonal cycles (Figure S3a in Supporting Information S1) (Martens et al., 2017). Based on the two relationships, we formulated an exponential function to characterize the correlation between GLEAM soil moisture and CH₄ flux ($R^2 = 0.63$, Figure S3b in Supporting Information S1), then applied this correlation to the Sudd region to estimate emission intensities. We stress that this methodology is only applicable to tropical seasonally flooded regions since it emphasizes the impact of soil water variations.

3. Results and Discussion

3.1. Evaluations of Our Reconstructed Wetland Area

We evaluated the estimated wetland extent on both grid and regional levels. For the grid level, our reconstructed maps can reproduce the spatial patterns and temporal dynamics of observation-based wetland extent well with RMSE <6% and $R^2 > 0.5$ in most (70%) grids (Figure S1c and S1d in Supporting Information S1), and the regionally averaged RMSE and R^2 are 3.6% and 0.61, respectively (Figure S1b in Supporting Information S1). Considering that some areas in the Sudd region are devoid of seasonally flooded wetlands (e.g., grids in the southwestern highland area of the Sudd region), we re-evaluated the performance of our statistic model in wetland-dominated grids (averaged wetland fraction >20% in Berkeley-RWAWC data). The modified averaged R^2 increases to 0.67, suggesting the effectiveness of our model to simulate wetland dynamics on the grid level. Figure S4 in Supporting Information S1 compares the spatial patterns of reconstructed and observed wetland extents in April and October for 2019–2022, which typically represent the periods of minimum and maximum extent of wetland area in the Sudd region. Compared with the Berkeley-RWAWC product, our reconstruction can reproduce the spatial patterns of observation-based wetland extent well in most (70%) grids with discrepancies of <3% for April and <6% for October, suggesting that our model can reproduce the large variations of the inundation area.

For the regional level, the total wetland area over the Sudd region of our reconstruction presents a good consistency with the Berkeley-RWAWC products (RMSE = 10% and $R^2 = 0.93$, Figure 2a). Our reconstruction shows an annual total wetland extent of $5.73 \pm 2.05 \times 10^4$ km² (mean ± 1σ) for 2003–2022, with an average growth rate of 7.93×10^2 km² yr⁻¹ (Figure 2a). The seasonal cycle of the total wetland area has a 2–3 months delay compared to that of regional precipitation (Figure 2b), which is consistent with previous analysis using ERA5 precipitation (Gerlein-Safdi et al., 2021). Importantly, our reconstruction provides a 20-year monthly continuous wetland extent time series at a resolution of 0.5° × 0.5° across the Sudd region, which could help wetland CH₄ emission estimation there.

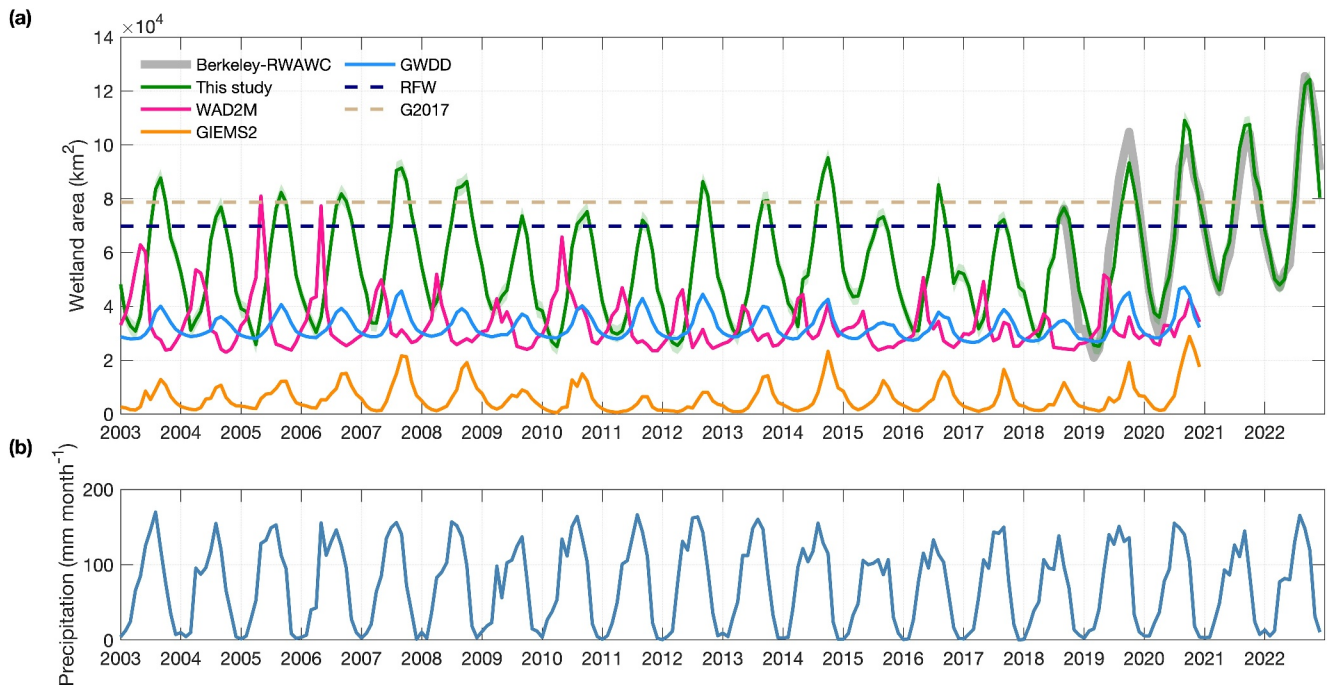


Figure 2. (a) Comparison between the simulated wetland area and other wetland extent products. Shaded areas of the simulation of this study represent one standard deviation of uncertainty. The time series of the Global Wetland Dynamics Dataset (GWDD) is the mean value of 28 simulations. (b) Monthly precipitation from Multi-Source Weighted-Ensemble Precipitation (MSWEP) averaged across the Sudd region.

3.2. Comparison With Existing Wetland Extent Products

We compared our reconstructed wetland maps to four widely used wetland area data sets, including Wetland Area and Dynamics for Methane Modeling (WAD2M) (Z. Zhang et al., 2021a), Global Inundation Estimate from Multiple Satellites version 2 (GIEMS-2) (Prigent et al., 2020), the Regularly Flooded Wetland map (RFW) (Tootchi et al., 2018) and the pantropical wetland extent from an expert system model (named G2017 according to its reference) (Gumbricht et al., 2017). Among them, WAD2M and GIEMS-2 include monthly time series, while RFW and G2017 are static maps. Additionally, we also included a Global Wetland Dynamics Dataset (GWDD) that provides an ensemble of monthly wetland extent simulations based on the Topography-based Hydrological Model (TOPMODEL) and calibrated with four satellite-derived wetland data mentioned above (Xi et al., 2021).

Overall, our reconstructed wetland extent in the Sudd region shows larger annual areas and amplitude of seasonal cycles compared with other wetland products (Figure 2a). The averaged total extent is 1.7, 5.3, and 1.7 times larger than those for WAD2M, GIEMS-2, and GWDD, respectively. These discrepancies are primarily evident in the flooded season, where the average maximum areas for our results are 1.6–3.5 times larger than those for other monthly integrated products, while the annual minimum area of different products is close. Compared with two static wetland maps that represent the long-term maximum area, from 2003 to 2022, the maximum values of most years in our reconstructed time series are higher than those for RFW and G2017. This is due to the omission of seasonally inundated areas on the eastern bank of the White Nile for RFW, while alongside the river channel for G2017 (Figure S5 in Supporting Information S1). Despite the potential overestimation of the CYGNSS-detected surface water (Downs et al., 2023), the benchmark data (Berkeley-RWAWC) of our estimation presents a high degree of consistency with river water levels, LWE, and GIEMS-2 product in terms of the seasonal cycle (Figures 1d and 2a), indicating a capacity to better capture the temporal dynamics of wetland extent.

It is noteworthy that the seasonal cycle of WAD2M, which is an improved version of the Surface Water Microwave Product Series (SWAMPS) product (Jensen & McDonald, 2019), usually indicates the maximum wetland extent during dry seasons and the minimum wetland extent during flooding seasons, being out of phase with other wetland data sets (Figure 2a). This mismatch may arise from the constrained capability of products based on passive microwave bands (e.g., SWAMPS) to detect seasonal inundation outside river floodplains, as well as from temporal inconsistencies among multiple data sources utilized for data fusion

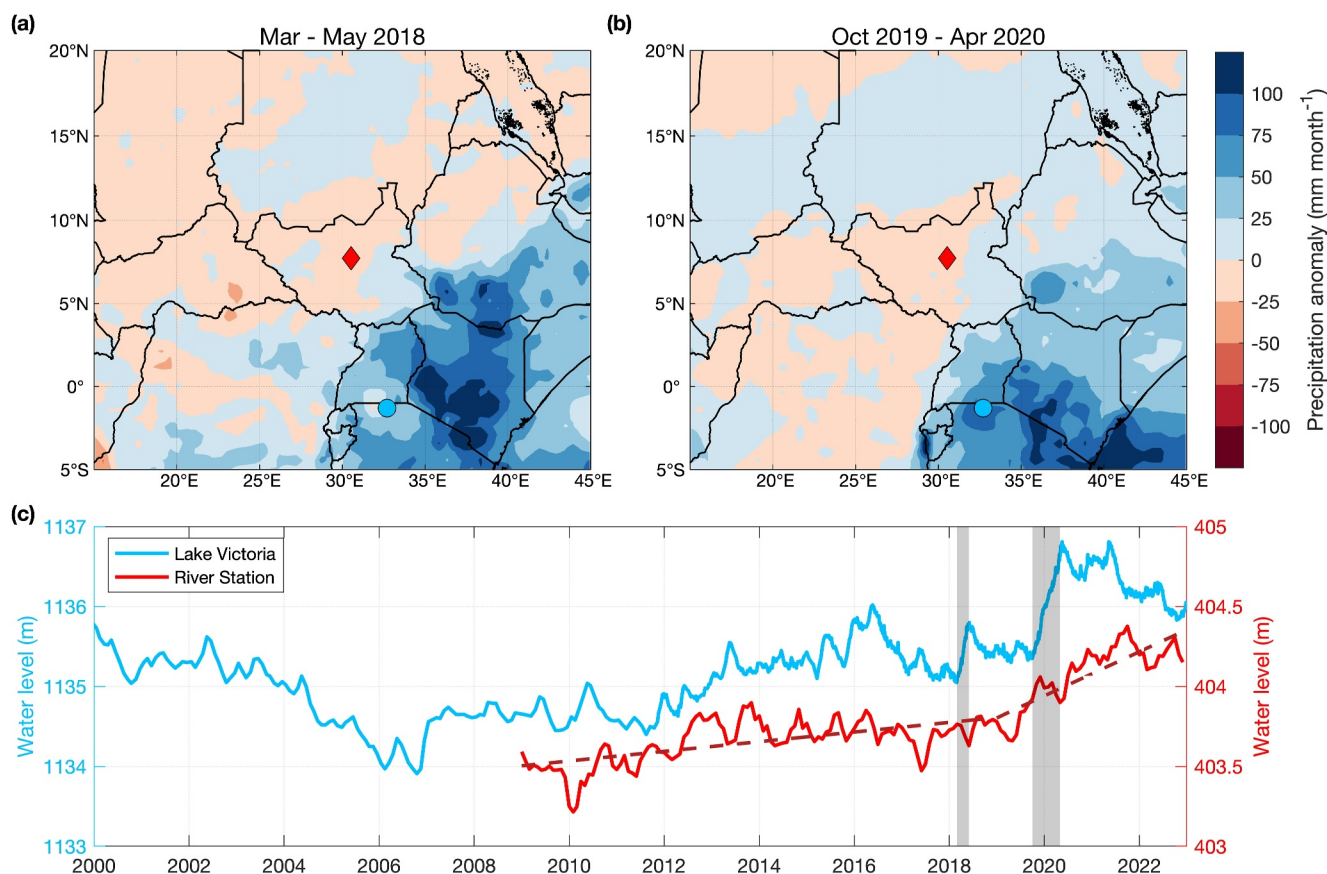


Figure 3. (a–b) Spatial patterns of precipitation anomalies in March–May 2018 and October 2019–April 2020. (c) Comparison of the water level of Lake Victoria (marked with blue circles in (a) and (b)) and a virtual station of the White Nile (marked with red diamonds in (a) and (b)). The time series of river water level (based on satellite altimetry) is calculated by a 3-month moving average. Gray vertical bars represent two special periods highlighted in (a) and (b). Dashed lines indicate the linear regression results for 2009–2018 and 2019–2022.

(Z. Zhang et al., 2021a). Given the prevalent utilization of the WAD2M product for wetland CH₄ emissions estimations (Bloom et al., 2017; McNicol et al., 2023b; Saunois et al., 2020a), like the Sudd wetland, we highlight its potential shortcoming over tropical floodplains.

3.3. Expansion of Wetland Area for 2019–2022 Driven by Upstream Precipitation

We detected an abrupt shift in the total wetland area time series around 2019, with no significant change from 2003 to 2018 (slope = $-69 \text{ km}^2 \text{ yr}^{-1}$, $P = 0.80$), but a significant increase from 2019 to 2022 (slope = $1.19 \times 10^4 \text{ km}^2 \text{ yr}^{-1}$, $P < 0.01$) (Figure S6 in Supporting Information S1). This increase can mainly be attributed to wetland-dominated grids where the average increase rate of wetland fraction is $\sim 6\% \text{ yr}^{-1}$ (Figure S7 in Supporting Information S1). The total wetland extent of the period 2019–2022 shows a 28% increase from the pre-2019 level, which is consistent with previous findings based on 3-month Landsat composites, but for smaller magnitudes (Hardy et al., 2023).

Normally, wetland extent tends to increase with rising water levels as expanded water bodies inundate surrounding areas, promoting wetland formation and expansion. The increasing trend from 2019 to 2022 is also detected in satellite-derived water height anomalies (methods described by Normandin et al. (2018)) of the White Nile from two virtual stations located at the central part (slope = 0.14 m yr^{-1} , $P < 0.01$) (Figure 3c) and downstream outlet (slope = 0.53 m yr^{-1} , $P < 0.01$) of the Sudd wetland (Figure 1d), indicating an elevation of total water inflow that could be attributed to the rise in regional precipitation or/and upstream discharge.

From 2018 to 2020, we observe a significant rise (slope = 0.48 m yr^{-1} , $P < 0.01$) in the water level of Lake Victoria, characterized by two abrupt rises during early 2018 and late 2019 that aligned with positive precipitation

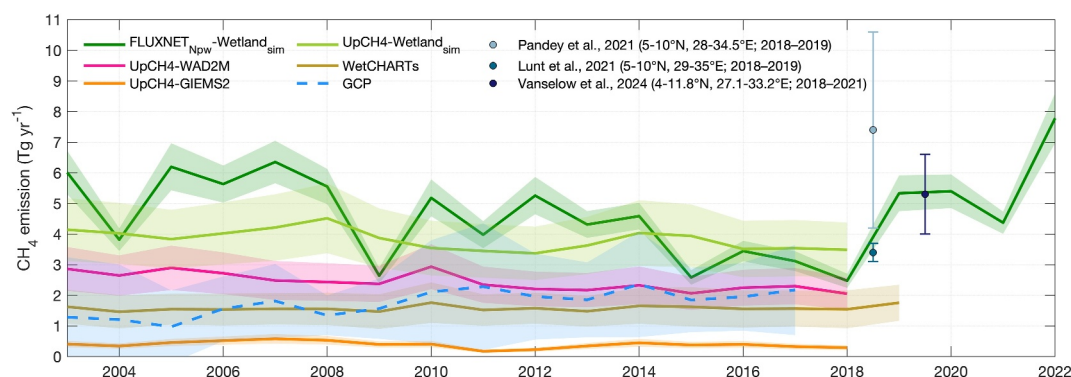


Figure 4. Comparison between the simulated wetland CH₄ emissions and other estimations. Shaded areas and error bars represent one standard deviation of uncertainty. Bottom-up and top-down estimations are distinguished by solid lines and dashed lines, respectively. Note that data from Pandey et al. (2021), Lunt et al. (2021), and Vanselow et al. (2024) are calculated using different region definitions, but all cover the emission hotspot areas in the Sudd wetland.

anomalies in the surrounding region (Figure 3). The extreme precipitation elevated Lake Victoria's water levels and increased the flow of other sources that feed the White Nile, which could amplify downstream flows toward the Sudd region, thereby expanding the extent of wetlands. Although the water level of Lake Victoria dropped in 2021, its outflow remained at a relatively high level according to the relationship fitted by the Agreed Curve (Sutcliffe & Petersen, 2007), leading to the continued expansion of the wetland area in 2021 and 2022. Considering the fact that no evident change in regional precipitation (slope = 3.12 mm yr⁻¹, $P = 0.66$) was detected during 2019–2022 (Figure 2b), we attribute the rapid growth of wetland extent to the precipitation anomalies in the upstream area of the Sudd wetland. The strong precipitation anomalies in East Africa for 2019–2020 could be associated with the extremely positive index of the Indian Ocean Dipole (Wainwright et al., 2021). Present wetland process models mostly rely on local precipitation to drive wetland extent (Bloom et al., 2017), and even the TOPMODEL could miss the wetlands and/or place wetlands in the wrong location due to complex river network and topography (Parker et al., 2022). Here we highlight that the influence of upstream precipitation is important for the Sudd wetland and the process of fluvial inundation is needed in future model developments.

3.4. CH₄ Emissions in the Sudd Wetland

Figure 4 shows the comparison of the annual wetland CH₄ emissions between our estimates and other bottom-up (BU) and top-down (TD) estimates. Our site-based estimation presents the largest averaged annual emissions (4.7 ± 1.4 Tg yr⁻¹), followed by the estimation based on the combination of our reconstructed area and UpCH4 wetland emission intensity (3.8 ± 0.3 Tg yr⁻¹). This difference could be attributed to UpCH4 integrating predictions from other non-floodplain sites, which might mitigate the impact of WTD fluctuations. The estimation of CH₄ emissions exhibits a high sensitivity to wetland extent, with the averaged annual emissions estimates for WAD2M and GIEMS-2 only amounting to 52%–64% and 5%–14% of that derived from our wetland extent, respectively (Figure 4). In contrast, CH₄ emissions are less sensitive to wetland emission intensities calculated by different approaches, as the uncertainties of our site-based estimation mostly overlap with those for UpCH4 when using the same extent. This further underscores the dominant role of wetland area dynamics in CH₄ emissions. According to our site-based estimation, during 2019–2022, the rapid growth of wetland extent resulted in a sharp increase in wetland CH₄ emissions (trend = 0.63 Tg yr⁻²), with the annual emission amount reaching 7.8 ± 0.8 Tg yr⁻¹ in 2022. This could partly contribute to the recent rise in atmospheric CH₄ growth rate from an average of 5.5 ppb yr⁻¹ during 2003–2018 to 14.0 ppb yr⁻¹ during 2019–2022 (Lan et al., 2024).

For TD estimates, the global inversion from the Global Carbon Project (GCP) ensemble mean is 54%–63% lower than our BU estimations (Figure 4). Although two regional inversions from the Tropospheric Monitoring Instrument (TROPOMI) are close to our BU estimates during the period 2018–2021 (Lunt et al., 2021; Vanselow et al., 2024), they encompass contributions from other emission sources (e.g., biomass burning, livestock, and rice paddy), which suggest lower wetland emissions. The underestimation of both global and regional inversions could be attributed to the underestimation from priori assumptions (e.g., WetCHARTs ensemble mean used in regional inversions) and the sparse data coverage in the tropics when surface observations are used as constraints

(Figure 4). Thus, we recommend priori derived from the wetland extent of Berkeley-RWAWC or our reconstruction for future TD inversions.

In this study, CH₄ emission intensities are estimated by WTD proxy (soil moisture), and this method entails considerable uncertainty due to the lack of observation on CH₄ fluxes and WTD in the Sudd region. Until now, due to data paucity, uncertainties in extrapolated CH₄ fluxes based on machine learning in tropical regions are still high (McNicol et al., 2023b). Moreover, generating a cohesive map of WTD and its temporal dynamics poses a considerable challenge (Reinecke et al., 2023). Hence, augmenting the network of CH₄ observation stations and expanding field data collections are expected to improve the accuracy of estimated wetland CH₄ emissions in the Sudd region, as well as other tropical seasonally flooded regions.

4. Conclusions

We developed a robust method for mapping long-term wetland extent across the Sudd wetland based on Berkeley-RWAWC inundation data, then utilized this data set to improve estimates of wetland CH₄ emissions. Annual total wetland areas are estimated to be $5.42 \pm 1.76 \times 10^4$ km² for 2003–2018 and increased to $6.95 \pm 2.63 \times 10^4$ km² for 2019–2022 driven by the anomalous precipitation in the upstream area. The shift in wetland extent leads to an increase in wetland CH₄ emissions from 4.1 ± 0.8 Tg yr⁻¹ for 2003–2018 to 5.7 ± 1.5 Tg yr⁻¹ for 2019–2022, which are larger than other BU/TD estimates using products with smaller wetland area. Our results suggest the important role of refined wetland extent products in estimating CH₄ emissions across tropical flooded areas.

Conflict of Interest

The authors declare no conflicts of interest relevant to this study.

Data Availability Statement

The Berkeley-RWAWC inundation data product is available at <https://doi.org/10.5067/CYGNS-L3W31> (CYGNSS, 2024). The GRACE/GRACE-FO Mascon data are available at <http://grace.jpl.nasa.gov> (Landerer et al., 2020). The MSWEP v2.8 precipitation data are available at <https://www.gloh2o.org/mswep> (Beck et al., 2019). The time series of water levels in the rivers and lakes are available at https://doi.org/10.24400/329360/HYDROWEB_WATER_LEVEL (HYDROWEB, 2023). The GLEAM v3.8a root-zone soil moisture data are available at <https://www.gleam.eu> (Martens et al., 2017). The FLUXNET-CH4 data for the site Northern Pantanal Wetland (BR-Npw) are available at <https://doi.org/10.18140/FLX/1669368> (Vourlitis et al., 2020). The WAD2M v2.0 wetland extent product is available at <https://doi.org/10.5281/zenodo.5553187> (Z. Zhang et al., 2021b). The GIEMS-2 wetland extent product (Prigent et al., 2020) is available at request from Catherine Prigent (catherine.prigent@obspm.fr). The GWDD wetland extent product is available at <https://doi.org/10.5281/zenodo.4571667> (Xi et al., 2021). The RFW wetland map is available at <https://doi.org/10.1594/PANGAEA.892657> (Tootchi et al., 2018). The G2017 wetland map (Gumbrecht et al., 2017) is available at request from Rosa Maria Roman-Cuesta (rosa.roman@wur.nl). The UpCH4 CH₄ flux outputs are available at <https://doi.org/10.3334/ORNLDAAAC/2253> (McNicol et al., 2023a). The WetCHARTs v1.3.1 data set is available at <https://doi.org/10.3334/ORNLDAAAC/1915> (Bloom et al., 2021). The GCP methane budget data set is available at <https://doi.org/10.18160/GCP-CH4-2019> (Saunio et al., 2020b).

References

- Beck, H. E., Wood, E. F., Pan, M., Fisher, C. K., Miralles, D. G., Van Dijk, A. I. J. M., et al. (2019). MSWEP V2 global 3-hourly 0.1° precipitation: Methodology and quantitative assessment. *Bulletin of the American Meteorological Society*, 100(3), 473–500. <https://doi.org/10.1175/BAMS-D-17-0138.1>
- Bloom, A. A., Bowman, K. W., Lee, M., Turner, A. J., Schroeder, R., Worden, J. R., et al. (2017). A global wetland methane emissions and uncertainty dataset for atmospheric chemical transport models (WetCHARTs version 1.0). *Geoscientific Model Development*, 10(6), 2141–2156. <https://doi.org/10.5194/gmd-10-2141-2017>
- Bloom, A. A., Bowman, K. W., Lee, M., Turner, A. J., Schroeder, R., Worden, J. R., et al. (2021). CMS: Global 0.5-deg Wetland Methane Emissions and Uncertainty (WetCHARTs v1.3.1) [Dataset]. *ORNL DAAC*. <https://doi.org/10.3334/ORNLDAAAC/1915>
- Chew, C., Small, E., & Huelsing, H. (2023). Flooding and inundation maps using interpolated CYGNSS reflectivity observations. *Remote Sensing of Environment*, 293, 113598. <https://doi.org/10.1016/j.rse.2023.113598>
- CYGNSS. (2024). UC Berkeley CYGNSS Level 3 Monthly RWAWC Watermask Version 3.1 [Dataset]. *NASA Physical Oceanography Distributed Active Archive Center*. <https://doi.org/10.5067/CYGNS-L3W31>

Acknowledgments

This work was supported by the National Natural Science Foundation of China (Grant 42325102), and by the National Key Research and Development Program of China under Grant 2022YFE0209100. Cynthia Gerlein-Safdi and Tianjiao Pu were supported by the National Aeronautics and Space Administration under Grant 80NSSC21K100. We thank Thomas Gumbrecht and Rosa Maria Roman-Cuesta for sharing the tropical wetland map.

- Downs, B., Kettner, A. J., Chapman, B. D., Brakenridge, G. R., O'Brien, A. J., & Zuffada, C. (2023). Assessing the relative performance of GNSS-R flood extent observations: Case study in south Sudan. *IEEE Transactions on Geoscience and Remote Sensing*, *61*, 1–13. <https://doi.org/10.1109/TGRS.2023.3237461>
- Feng, L., Palmer, P. I., Zhu, S., Parker, R. J., & Liu, Y. (2022). Tropical methane emissions explain large fraction of recent changes in global atmospheric methane growth rate. *Nature Communications*, *13*(1), 1378. <https://doi.org/10.1038/s41467-022-28989-z>
- Gerlein-Safdi, C., Bloom, A. A., Plant, G., Kort, E. A., & Ruf, C. S. (2021). Improving representation of tropical wetland methane emissions with CYGNSS inundation maps. *Global Biogeochemical Cycles*, *35*(12), e2020GB006890. <https://doi.org/10.1029/2020GB006890>
- Gerlein-Safdi, C., & Ruf, C. S. (2019). A CYGNSS-based algorithm for the detection of inland waterbodies. *Geophysical Research Letters*, *46*(21), 12065–12072. <https://doi.org/10.1029/2019GL085134>
- Gou, J., & Soja, B. (2024). Global high-resolution total water storage anomalies from self-supervised data assimilation using deep learning algorithms. *Nature Water*, *2*(2), 139–150. <https://doi.org/10.1038/s44221-024-00194-w>
- Gumbrecht, T., Roman-Cuesta, R. M., Verchot, L., Herold, M., Wittmann, F., Householder, E., et al. (2017). An expert system model for mapping tropical wetlands and peatlands reveals South America as the largest contributor. *Global Change Biology*, *23*(9), 3581–3599. <https://doi.org/10.1111/gcb.13689>
- Hardy, A., Palmer, P. I., & Oakes, G. (2023). Satellite data reveal how Sudd wetland dynamics are linked with globally-significant methane emissions. *Environmental Research Letters*, *18*(7), 074044. <https://doi.org/10.1088/1748-9326/ace272>
- HYDROWEB. (2023). Water levels of rivers and lakes [Dataset]. *Theia Hydroweb*. https://doi.org/10.24400/329360/HYDROWEB_WATER_LEVEL
- IPCC. (2021). *Climate Change 2021 – The Physical Science Basis: Working Group I Contribution to the Sixth Assessment Report of the Intergovernmental Panel on Climate Change* (1st ed.). Cambridge University Press. <https://doi.org/10.1017/9781009157896>
- Jensen, K., & McDonald, K. (2019). Surface water microwave product series version 3: A near-real time and 25-year historical global inundated area fraction time series from active and passive microwave remote sensing. *IEEE Geoscience and Remote Sensing Letters*, *16*(9), 1402–1406. <https://doi.org/10.1109/LGRS.2019.2898779>
- Kirschke, S., Bousquet, P., Ciais, P., Saunois, M., Canadell, J. G., Dlugokencky, E. J., et al. (2013). Three decades of global methane sources and sinks. *Nature Geoscience*, *6*(10), 813–823. <https://doi.org/10.1038/ngeo1955>
- Lan, X., Thoning, K., Dlugokencky, E., & NOAA Global Monitoring Laboratory. (2024). Trends in globally-averaged CH₄, N₂O, and SF₆ [Dataset]. *NOAA Global Monitoring Laboratory*. <https://doi.org/10.15138/P8XG-AA10>
- Landerer, F. W., Flechtner, F. M., Save, H., Webb, F. H., Bandikova, T., Bertiger, W. I., et al. (2020). Extending the global mass change data record: GRACE Follow-On instrument and science data performance. *Geophysical Research Letters*, *47*(12), e2020GL088306. <https://doi.org/10.1029/2020GL088306>
- Lehner, B., Anand, M., Fluet-Chouinard, E., Tan, F., Aires, F., Allen, G. H., et al. (2024). Mapping the world's inland surface waters: An update to the Global Lakes and Wetlands Database (GLWD v2). *Earth System Science Data Discussions*, 1–49. <https://doi.org/10.5194/essd-2024-204>
- Lunt, M. F., Palmer, P. I., Feng, L., Taylor, C. M., Boesch, H., & Parker, R. J. (2019). An increase in methane emissions from tropical Africa between 2010 and 2016 inferred from satellite data. *Atmospheric Chemistry and Physics*, *19*(23), 14721–14740. <https://doi.org/10.5194/acp-19-14721-2019>
- Lunt, M. F., Palmer, P. I., Lorente, A., Borsdorff, T., Landgraf, J., Parker, R. J., & Boesch, H. (2021). Rain-fed pulses of methane from East Africa during 2018–2019 contributed to atmospheric growth rate. *Environmental Research Letters*, *16*(2), 024021. <https://doi.org/10.1088/1748-9326/abd8fa>
- Martens, B., Miralles, D. G., Lievens, H., van der Schalie, R., de Jeu, R. A. M., Fernández-Prieto, D., et al. (2017). GLEAM v3: Satellite-based land evaporation and root-zone soil moisture. *Geoscientific Model Development*, *10*(5), 1903–1925. <https://doi.org/10.5194/gmd-10-1903-2017>
- Martins, V. S., Novo, E. M. L. M., Lyapustin, A., Aragão, L. E. O. C., Freitas, S. R., & Barbosa, C. C. F. (2018). Seasonal and interannual assessment of cloud cover and atmospheric constituents across the Amazon (2000–2015): Insights for remote sensing and climate analysis. *ISPRS Journal of Photogrammetry and Remote Sensing*, *145*, 309–327. <https://doi.org/10.1016/j.isprsjprs.2018.05.013>
- McNicol, G., Fluet-Chouinard, E., Ouyang, Z., Knox, S., Zhang, Z., Aalto, T., et al. (2023a). Global Wetland Methane Emissions derived from FLUXNET and the UpCH4 Model, 2001-2018 [Dataset]. *ORNL DAAC*. <https://doi.org/10.3334/ORNLLDAAC/2253>
- McNicol, G., Fluet-Chouinard, E., Ouyang, Z., Knox, S., Zhang, Z., Aalto, T., et al. (2023b). Upscaling wetland methane emissions from the FLUXNET-CH4 Eddy covariance network (UpCH4 v1.0): Model development, network assessment, and budget comparison. *AGU Advances*, *4*(5), e2023AV000956. <https://doi.org/10.3334/ORNLLDAAC/2253>
- Mekonnen, K., Velpuri, N. M., Leh, M., Akpoti, K., Owusu, A., Tinonetsana, P., et al. (2023). Accuracy of satellite and reanalysis rainfall estimates over Africa: A multi-scale assessment of eight products for continental applications. *Journal of Hydrology: Regional Studies*, *49*, 101514. <https://doi.org/10.1016/j.ejrh.2023.101514>
- Normandin, C., Frappart, F., Diepkilé, A. T., Marieu, V., Mougin, E., Blarel, F., et al. (2018). Evolution of the performances of radar altimetry missions from ERS-2 to Sentinel-3A over the Inner Niger Delta. *Remote Sensing*, *10*(6), 833. <https://doi.org/10.3390/rs10060833>
- Pandey, S., Houweling, S., Lorente, A., Borsdorff, T., Tsvilidou, M., Bloom, A. A., et al. (2021). Using satellite data to identify the methane emission controls of South Sudan's wetlands. *Biogeosciences*, *18*(2), 557–572. <https://doi.org/10.5194/bg-18-557-2021>
- Parker, R. J., Boesch, H., McNorton, J., Comyn-Platt, E., Gloor, M., Wilson, C., et al. (2018). Evaluating year-to-year anomalies in tropical wetland methane emissions using satellite CH₄ observations. *Remote Sensing of Environment*, *211*, 261–275. <https://doi.org/10.1016/j.rse.2018.02.011>
- Parker, R. J., Wilson, C., Comyn-Platt, E., Hayman, G., Marthews, T. R., Bloom, A. A., et al. (2022). Evaluation of wetland CH₄ in the Joint UK Land Environment Simulator (JULES) land surface model using satellite observations. *Biogeosciences*, *19*(24), 5779–5805. <https://doi.org/10.5194/bg-19-5779-2022>
- Poulter, B., Bousquet, P., Canadell, J. G., Ciais, P., Pregon, A., Saunois, M., et al. (2017). Global wetland contribution to 2000–2012 atmospheric methane growth rate dynamics. *Environmental Research Letters*, *12*(9), 094013. <https://doi.org/10.1088/1748-9326/aa8391>
- Prigent, C., Jimenez, C., & Bousquet, P. (2020). Satellite-derived global surface water extent and dynamics over the last 25 years (GIEMS-2). *Journal of Geophysical Research: Atmospheres*, *125*(3), e2019JD030711. <https://doi.org/10.1029/2019JD030711>
- Pu, T., Gerlein-Safdi, C., Xiong, Y., Li, M., Kort, E. A., & Bloom, A. A. (2024). Berkeley-RWAWC: A new CYGNSS-based watermask unveils unique observations of seasonal dynamics in the tropics. *Water Resources Research*, *60*(7), e2024WR037060. <https://doi.org/10.1029/2024WR037060>
- Reinecke, R., Gnann, S., Stein, L., Bierkens, M., de Graaf, I., Gleeson, T., et al. (2023). Considerable gaps in our global knowledge of potential groundwater accessibility. Retrieved from <https://eartharxiv.org/repository/view/5003/>

- Ruf, C. S., Chew, C., Lang, T., Morris, M. G., Nave, K., Ridley, A., & Balasubramaniam, R. (2018). A new paradigm in earth environmental monitoring with the CYGNSS small satellite constellation. *Scientific Reports*, 8(1), 8782. <https://doi.org/10.1038/s41598-018-27127-4>
- Saunoy, M., Stavert, A. R., Poulter, B., Bousquet, P., Canadell, J. G., Jackson, R. B., et al. (2020a). The global methane budget 2000–2017. *Earth System Science Data*, 12(3), 1561–1623. <https://doi.org/10.5194/essd-12-1561-2020>
- Saunoy, M., Stavert, A. R., Poulter, B., Bousquet, P., Canadell, J. G., Jackson, R. B., et al. (2020b). Supplemental data of the Global Carbon Project Methane Budget 2019 (Version 2.0) [Dataset]. *Global Carbon Project*. <https://doi.org/10.18160/GCP-CH4-2019>
- Shen, L., Mickley, L. J., & Murray, L. T. (2017). Influence of 2000–2050 climate change on particulate matter in the United States: Results from a new statistical model. *Atmospheric Chemistry and Physics*, 17(6), 4355–4367. <https://doi.org/10.5194/acp-17-4355-2017>
- Sutcliffe, J. V., & Parks, Y. P. (1999). *The hydrology of the Nile*. IAHS Press.
- Sutcliffe, J. V., & Petersen, G. (2007). Lake Victoria: Derivation of a corrected natural water level series Lac Victoria: dérivation d'une série naturelle corrigée des niveaux d'eau. *Hydrological Sciences Journal*, 52(6), 1316–1321. <https://doi.org/10.1623/hysj.52.6.1316>
- Tapley, B. D., Bettadpur, S., Watkins, M., & Reigber, C. (2004). The gravity recovery and climate experiment: Mission overview and early results. *Geophysical Research Letters*, 31(9), L09607. <https://doi.org/10.1029/2004GL019920>
- Tapley, B. D., Watkins, M. M., Flechtner, F., Reigber, C., Bettadpur, S., Rodell, M., et al. (2019). Contributions of GRACE to understanding climate change. *Nature Climate Change*, 9(5), 358–369. <https://doi.org/10.1038/s41558-019-0456-2>
- Tootchi, A., Jost, A., & Ducharme, A. (2018). Multi-source global wetland maps combining surface water imagery and groundwater constraints [Dataset]. *Sorbonne Université, Paris, France. PANGAEA*. <https://doi.org/10.1594/PANGAEA.892657>
- Vanselow, S., Schneising, O., Buchwitz, M., Reuter, M., Bovensmann, H., Boesch, H., & Burrows, J. P. (2024). Automated detection of regions with persistently enhanced methane concentrations using Sentinel-5 Precursor satellite data. <https://doi.org/10.5194/egusphere-2024-379>
- Vourlitis, G., Dalmagro, H., De, S., Nogueira, J., Johnson, M., & Arruda, P. (2020). FLUXNET-CH4 BR-Npw Northern Pantanal Wetland [Dataset]. *FLUXNET*. <https://doi.org/10.18140/FLX/1669368>
- Wainwright, C. M., Finney, D. L., Kilavi, M., Black, E., & Marsham, J. H. (2021). Extreme rainfall in East Africa, October 2019–January 2020 and context under future climate change. *Weather*, 76(1), 26–31. <https://doi.org/10.1002/wea.3824>
- Xi, Y., Peng, S., Ducharme, A., Ciais, P., Gumbrecht, T., Jimenez, C., et al. (2021). Dynamics of global wetlands by TOPMODEL (Version v3) [Dataset]. *Zenodo*. <https://doi.org/10.5281/zenodo.4571667>
- Yi, S., & Sneeuw, N. (2021). Filling the data gaps within GRACE missions using singular spectrum analysis. *Journal of Geophysical Research: Solid Earth*, 126(5), e2020JB021227. <https://doi.org/10.1029/2020JB021227>
- Zeiger, P., Frappart, F., Darrozes, J., Prigent, C., & Jiménez, C. (2022). Analysis of CYGNSS coherent reflectivity over land for the characterization of pan-tropical inundation dynamics. *Remote Sensing of Environment*, 282, 113278. <https://doi.org/10.1016/j.rse.2022.113278>
- Zhang, Y., He, B., Guo, L., & Liu, D. (2019). Differences in response of terrestrial water storage components to precipitation over 168 global river basins. *Journal of Hydrometeorology*, 20(9), 1981–1999. <https://doi.org/10.1175/JHM-D-18-0253.1>
- Zhang, Z., Fluet-Chouinard, E., Jensen, K., McDonald, K., Hugelius, G., Gumbrecht, T., et al. (2021a). Development of the global dataset of Wetland Area and Dynamics for Methane Modeling (WAD2M). *Earth System Science Data*, 13(5), 2001–2023. <https://doi.org/10.5194/essd-13-2001-2021>
- Zhang, Z., Fluet-Chouinard, E., Jensen, K., McDonald, K., Hugelius, G., Gumbrecht, T., et al. (2021b). Development of a global dataset of Wetland Area and Dynamics for Methane Modeling (WAD2M) (Version 2.0) [Dataset]. *Zenodo*. <https://doi.org/10.5281/zenodo.5553187>